

Supporting Information

Disentangling the Impact of Side Chains and Fluorine Substituents of Conjugated Donor Polymers on the Performance of Photovoltaic Blends

Liqiang Yang¹, John R. Tumbleston², Huaxing Zhou³, Harald Ade², and Wei You^{1,3,}*

1. Curriculum in Applied Sciences and Engineering, University of North Carolina at Chapel Hill,
Chapel Hill, North Carolina 27599-3287

2. Department of Physics, North Carolina State University, Raleigh, North Carolina 27695

3. Department of Chemistry, University of North Carolina at Chapel Hill, Chapel Hill, North
Carolina 27599-3290

* To whom all correspondence should be addressed. Email: wyou@unc.edu.

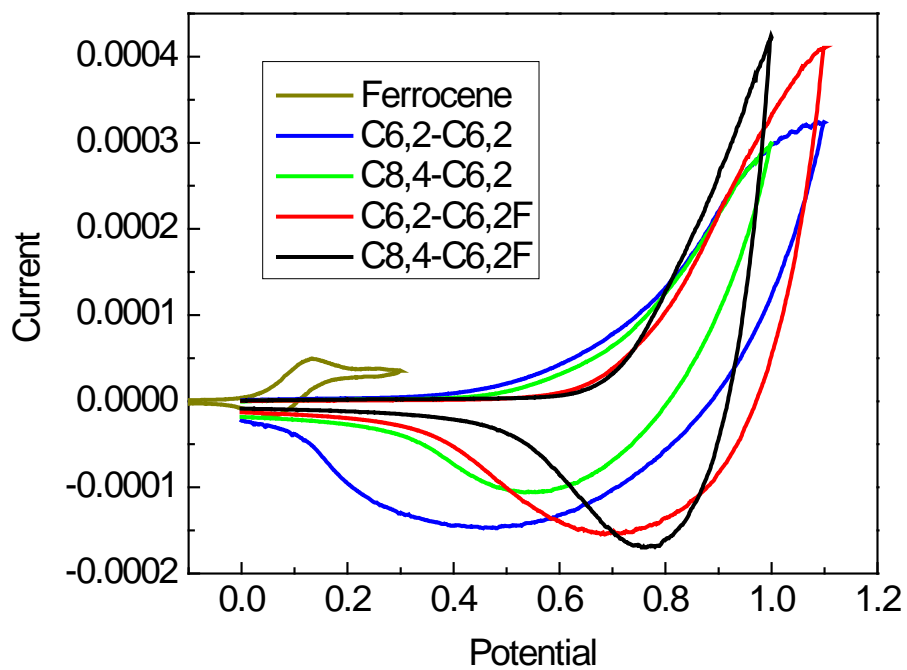


Figure S1 The oxidative portion of the cyclic voltammogram for polymer thin films. The ferrocene/ferrocenium redox couple is used as a standard (-4.8 eV).

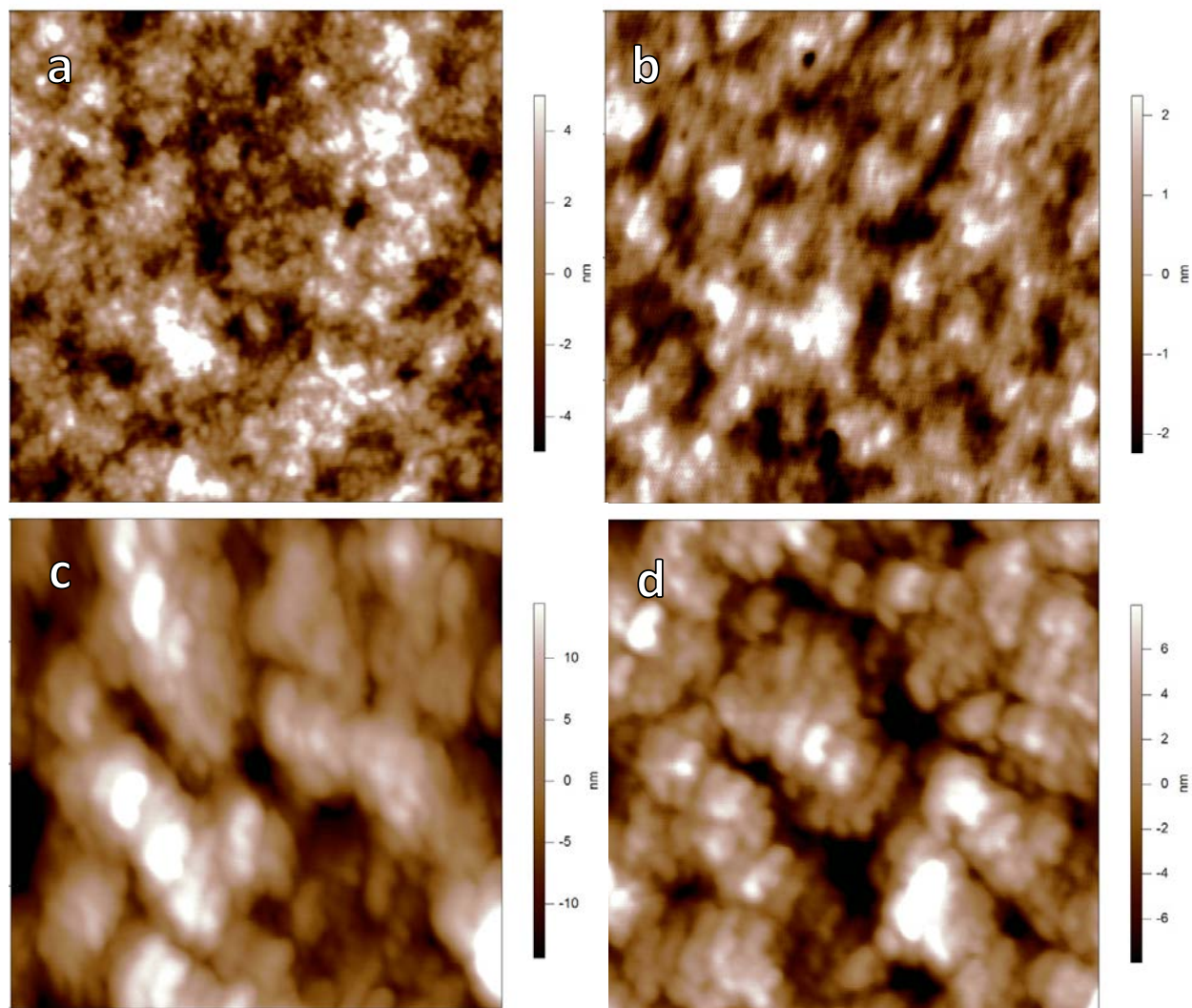


Figure S2. AFM height images ($2 \times 2 \mu\text{m}$) of (a) C6,2-C6,2, (b) C8,4-C6,2, (c) C6,2-C6,2F and (d) C8,4-C6,2F based BHJ devices.

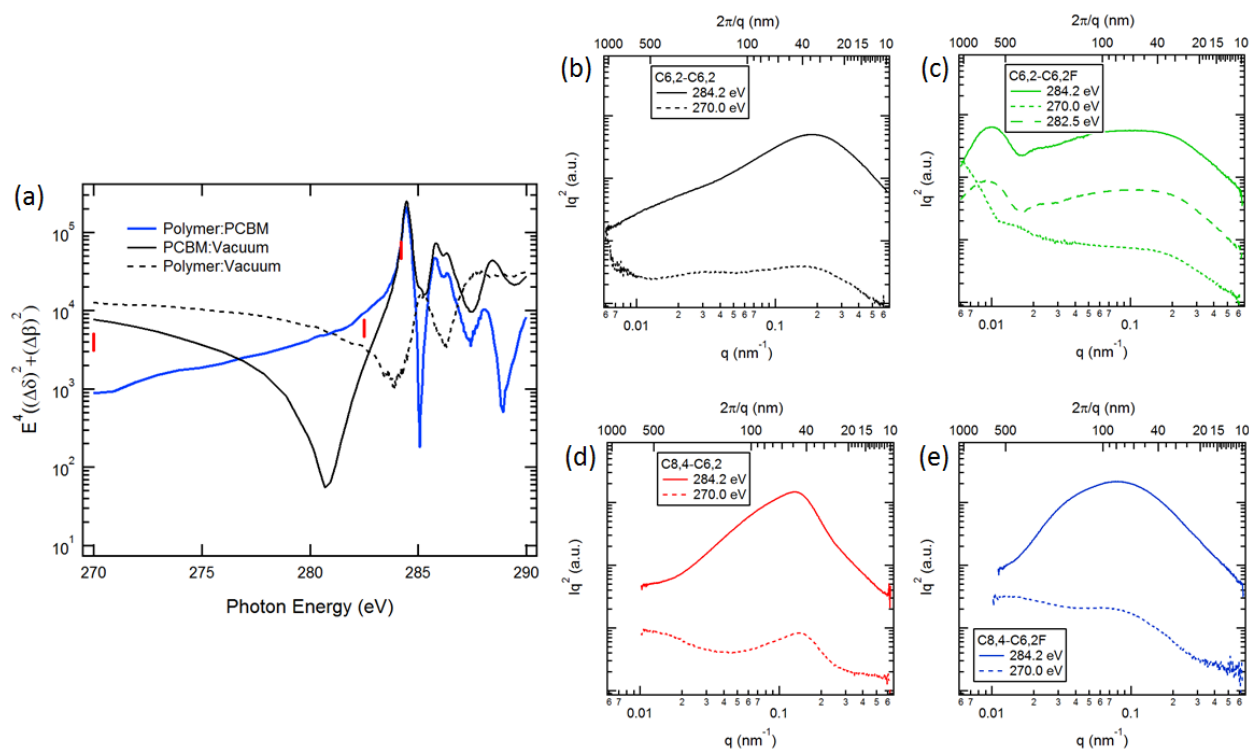


Figure S3. (a) Soft X-ray scattering contrast for polymer:PCBM as function of photon energy near the carbon 1s absorption edge. The imaginary part (β) of the optical constants ($n = 1 - \delta + i\beta$) of pure polymer and PCBM were measured with scanning transmission x-ray microscopy (STXM) at beamline 5.3.2.2 of the Advance Light Source.¹ The real part (δ) was then calculated with a Kramers-Kronig transformation assuming polymer and PCBM densities of 1.1 and 1.3 g/cm^3 , respectively. Significant differences in the optical constants were not found with variation of side chain or substituent atom. The scattering contrast is proportional to the difference squared of the real and imaginary parts. (b-e) R-SoXS 180° sector averages at 270 and 284.2 eV showing differences in scattering when vacuum (i.e. mass thickness) and materials contrast are selected, respectively. (c) There are only minimal differences between scattering profiles for 284.2 eV and 282.5 eV. For 282.5 eV, both the polymer and PCBM vacuum contrasts are minimized, which is the energy least sensitive to scattering due to surface roughness.

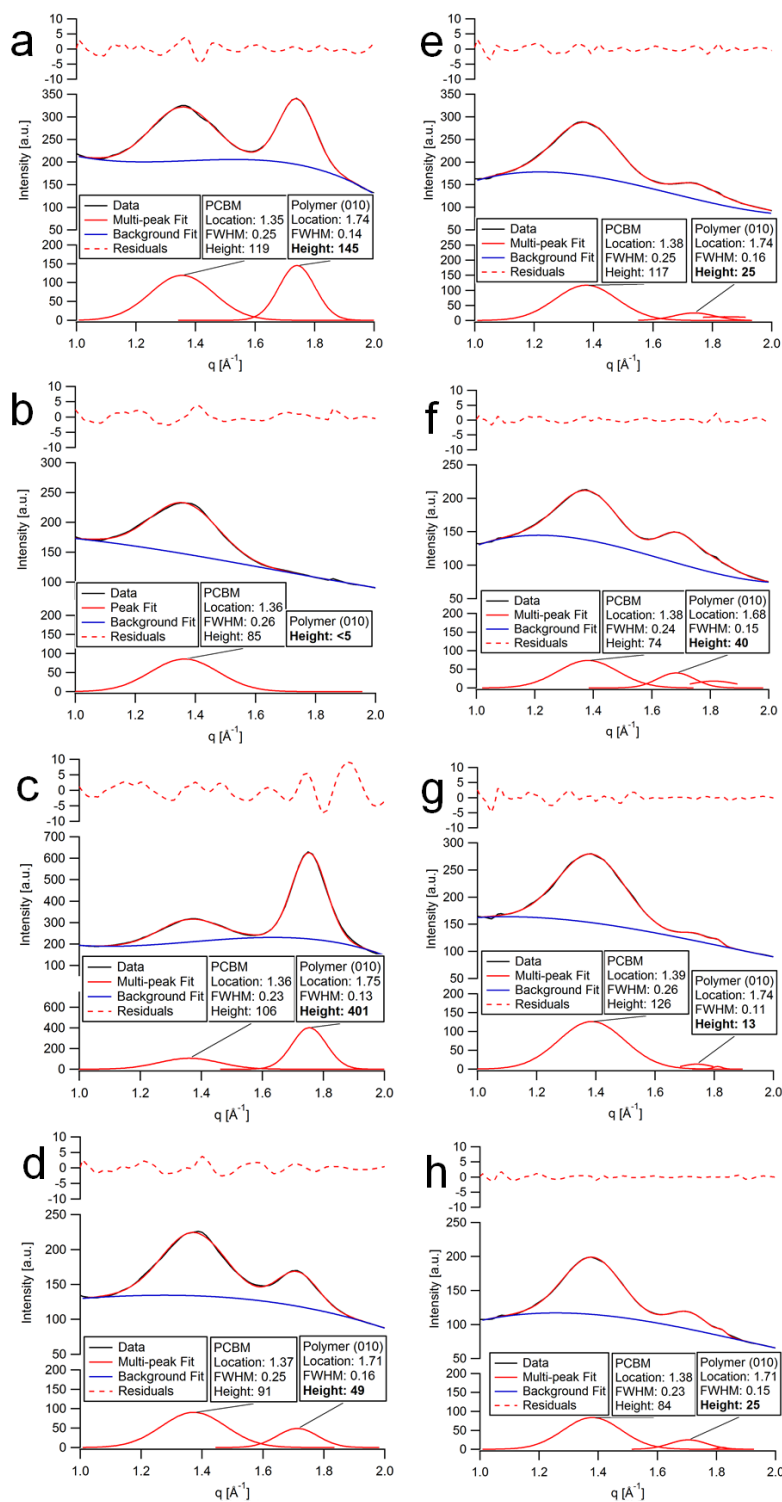


Figure S4. Multi-peak gaussian fitting to (a-d) out of plane and (e-h) in plane PCBM and polymer 010 peaks including fit residuals (dashed lines). A cubic background is simultaneously fit along with the q location, peak width, and height of each peak. For the in plane data, an additional peak near $q = 1.8 \text{ \AA}^{-1}$ is used. Panels (a,e) correspond to polymer/PCBM blend C6,2-C6,2, while (b,f) correspond to C8,4-C6,2, (c,g) C6,2-C6,2F, and (d,h) C8,4-C6,2F.

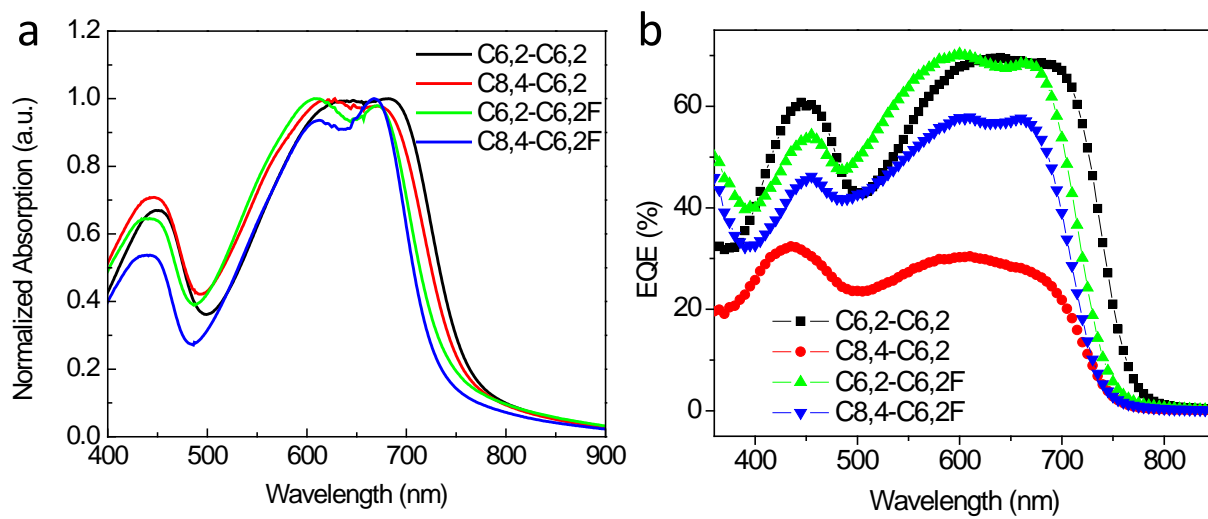


Figure S5. (a) Normalized absorption spectra of pure polymer thin films processed with dichlorobenzene; (b). EQE of devices based on four polymers.

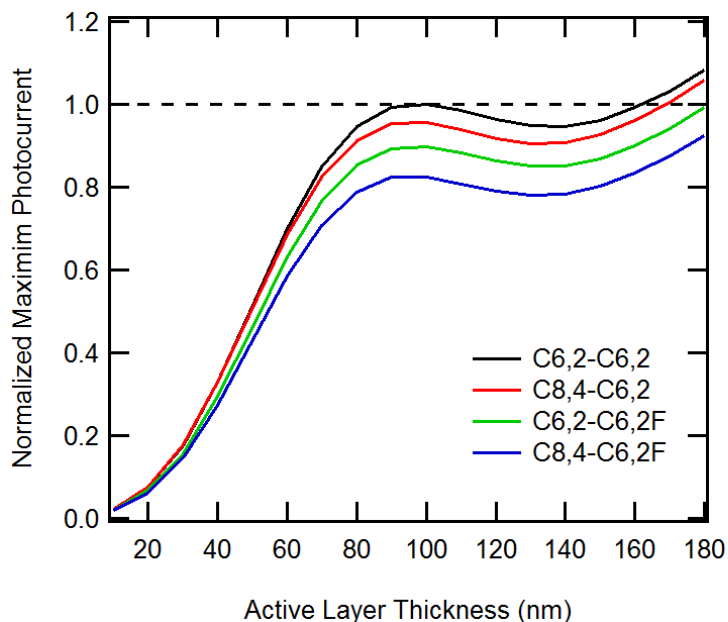


Figure S6. Normalized maximum photocurrent as function of active layer thickness for each polymer blend. The absorption coefficients from Figure 6b of the main text are used to calculate the imaginary part of the index of refraction, k , from $k = \alpha \cdot \lambda / 4\pi$, where α is the absorption coefficient and λ is the incident wavelength. The real part of the index of refraction for all wavelengths is then assumed to be 2.0, which has been shown to not significantly influence the overall absorption compared to using the true index dispersion.² Using the transfer matrix optical model, absorption in the active layer is then simulated using variable active layer thickness and the following device architecture: glass/ITO (150 nm)/PEDOT:PSS (40 nm)/active layer/aluminum. The optical properties of glass, ITO, PEDOT:PSS, and aluminum were measured using spectroscopic ellipsometry and are given elsewhere³ where the model accounts for parasitic absorption losses by the electrodes and optical interference due to each device interface. Absorption in the active layer is then convoluted with the standard 1 Sun solar spectrum and integrated between 350 and 875 nm to give a maximum achievable photocurrent assuming 100% internal quantum efficiency. These values are then normalized to the first peak of the C6,2-C6,2 polymer blend as shown above to compare how active layer thickness and differences in intrinsic absorption by each blend would affect the measured photocurrent, especially the short-circuit current.

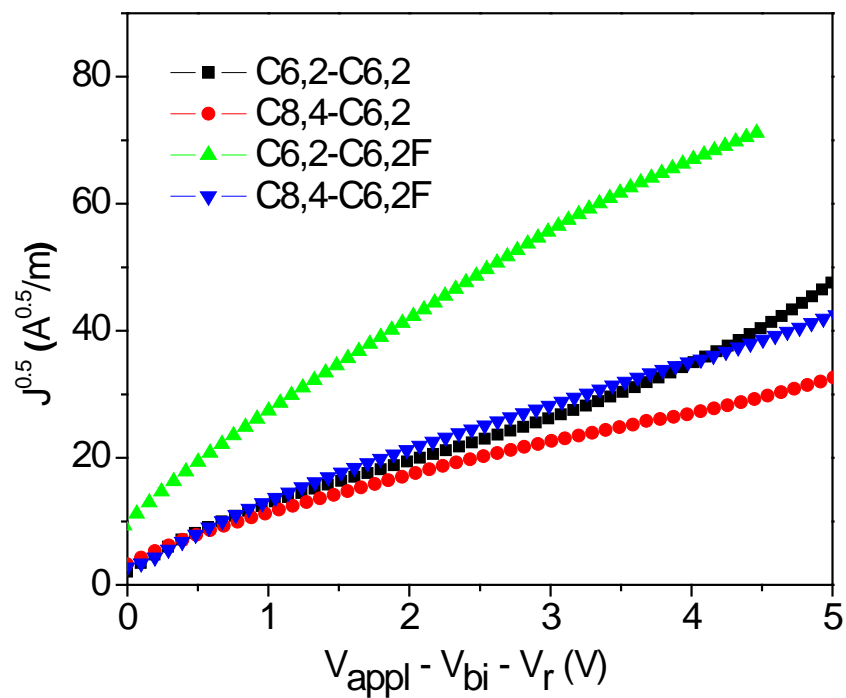


Figure S7. $J^{0.5}$ vs V plots for the polymer films at room temperature from a hole-only device of ITO/PEDOT:PSS (40 nm)/pure polymer or blend with PCBM/Pd (50 nm).

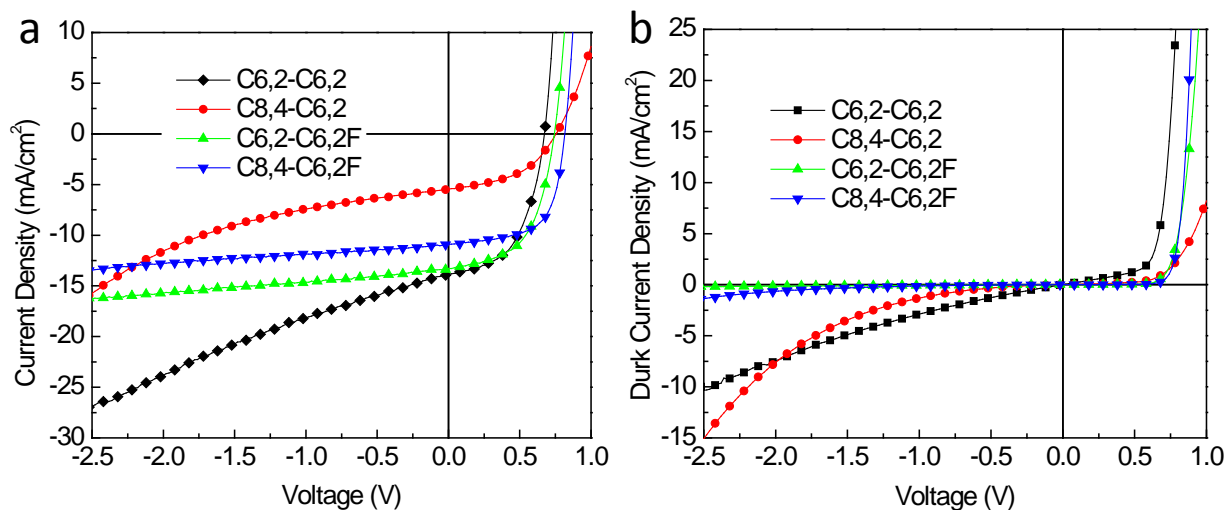


Figure S8. Current characteristics of BHJ solar cells under (a) 1 Sun illumination and (b) in the dark.

Reference:

- (1) Kilcoyne, A. L. D.; Tyliszczak, T.; Steele, W. F.; Fakra, S.; Hitchcock, P.; Franck, K.; Anderson, E.; Harteneck, B.; Rightor, E. G.; Mitchell, G. E.; Hitchcock, A. P.; Yang, L.; Warwick, T.; Ade, H. *J. Synchrotron Rad.* **2003**, *10*, 125.
- (2) Burkhard, G. F.; Hoke, E. T.; McGehee, M. D. *Adv. Mater.* **2010**, *22*, 3293.
- (3) Tumbleston, J. R.; Liu, Y.; Samulski, E. T.; Lopez, R. *Adv. Energy Mater.* **2012**, *2*, 477.